# Strongly Coupled Electroweak Symmetry Breaking: Implications of Models

R. Sekhar Chivukula,*
Rogerio Rosenfeld,
Elizabeth H. Simmons,
and John Terning

Department of Physics, Boston University,
590 Commonwealth Ave., Boston MA 02215

February 28, 1995

## Abstract

We discuss the phenomenology of models of dynamical electroweak symmetry breaking which attempt to generate the observed fermion mass spectrum. After briefly describing the variety of and constraints on proposed models, we concentrate on the signatures of colored pseudo-Nambu-Goldstone bosons and resonances at existing and proposed colliders. These particles provide a possibly unique signature: *strongly produced* resonances associated with *electroweak* symmetry breaking.

---

*e-mail: sekhar@bu.edu, rosenfeld@if.usp.br, simmons@smyrd.bu.edu, terning@calvin.bu.edu

# 1  Introduction

The standard $SU(2)_L \times U(1)_Y$ gauge theory of the electroweak interactions is in good agreement with all current experimental data. Nonetheless, there is no evidence to show which mechanism is responsible for the breakdown of this symmetry to the $U(1)$ of electromagnetism.

It is usually assumed that electroweak symmetry breaking (EWSB) is due to the vacuum expectation value of one or more fundamental scalars which are doublets of $SU(2)_L$. This explanation is unsatisfactory for a number of reasons:

• In all such theories there must be at least one physical degree of freedom remaining from the fundamental scalar doublet(s), the Higgs boson. As yet, there is no direct evidence for the existence of such a state.

• These models do not give a dynamical explanation of electroweak symmetry breaking. Instead, the potential must be adjusted to produce the desired result.

• When embedded in theories with additional dynamics at higher energy scales, these theories are technically unnatural [1]. For example, in the context of Grand Unified Theories (GUTs) radiative corrections to the Higgs boson mass(es) give contributions proportional to large (GUT-scale) masses. The Higgs mass must be "fine tuned" to be of order the weak scale.

• Theories of fundamental scalars are thought to be "trivial" [2], *i.e.* it is not possible to construct an interacting theory of scalars (in four dimensions) which is valid to arbitrarily short distance scales. Rather, a theory of scalars must be viewed as a low-energy effective theory. New physics must enter below the energy scale of the "Landau-pole" of the scalar theory.

This last consideration implies that, whether or not a Higgs boson exists, there must be new physics beyond the standard one-Higgs doublet model at some (possibly exponentially high) energy scale. In this sense, theories with a weakly coupled Higgs, including the ever-popular minimal supersymmetric standard model, simply allow one to postpone answering the question of what is responsible for electroweak symmetry breaking (and other related questions such as the origin of fermion masses) up to very high energies.

In theories of dynamical electroweak symmetry breaking, such as technicolor [3, 4], EWSB is due to chiral symmetry breaking in an asymptotically-free, strongly-interacting, gauge theory with massless fermions. Unlike theories with fundamental scalars, theories of dynamical EWSB are natural. Like the QCD scale, $\Lambda_{QCD}$, the weak scale arises by dimensional transmutation and can be exponentially smaller than, say, the GUT or Planck scales. Furthermore, non-Abelian gauge theories may make sense as fundamental theories.

In the simplest technicolor theory one introduces a left-handed weak-doublet of "technifermions", and the corresponding right-handed weak-singlets; both transform as $N$'s of a strong $SU(N)_{TC}$ technicolor gauge group. The global chiral symmetry respected by the strong technicolor interactions is $SU(2)_L \times SU(2)_R$.

When the technicolor interactions become strong, the chiral symmetry is broken to the diagonal subgroup, $SU(2)_V$, producing three Nambu-Goldstone bosons which become, via the Higgs mechanism, the longitudinal degrees of freedom of the $W$ and $Z$. Because the left-handed and right-handed techni-fermions carry different electroweak quantum numbers, the electroweak interactions break down to electromagnetism. If the $F$-constant of the theory, the analog of $f_\pi$ in QCD, is chosen to be 246 GeV, then the $W$ mass has its observed value. Furthermore, since the symmetry structure of the theory is *precisely* the same as that of the standard one Higgs-doublet model, the remaining $SU(2)_V$ "custodial" symmetry insures that $M_W = M_Z \cos\theta_W$.

In addition to the "eaten" Nambu-Goldstone bosons, such a theory will give rise to various resonances, the analogs of the $\rho$, $\omega$, and possibly the $\sigma$, in QCD. The phenomenology of an $SU(2)_L \otimes SU(2)_R \to SU(2)_V$ model in general, and of resonances of this sort in particular, are discussed in ref. 5. However, the symmetry breaking sector must also couple to the ordinary fermions, allowing them to acquire mass. In models of a strong electroweak symmetry breaking sector there must either be additional flavor-dependent gauge interactions [6, 7], the so-called "extended" technicolor (ETC) interactions, or Yukawa couplings to scalars [32] (as in the standard model) which communicate the breaking of the chiral symmetry of the technifermions to the ordinary fermions. The most popular type of strong EWSB model which attempts to explain the masses of all observed fermions contains an entire family of technifermions with standard model gauge couplings. Such models are referred to as one-family models. While this is a reasonable starting point for model building, given the family structure of the observed fermions, a variety of other possibilities have been explored.

Models containing more than one doublet of technifermions have a global symmetry group larger than $SU(2)_L \otimes SU(2)_R$. Therefore chiral symmetry breaking produces additional (pseudo-)Nambu-Goldstone bosons (PNGBs), other than those required to provide the longitudinal degrees of freedom of the $W$ and $Z$. Furthermore, the models typically possess a larger variety of resonances than the one-doublet model. The phenomenology of arbitrary color-neutral PNGBs and resonances is similar to that discussed in ref. 5 or, in the case of color-neutral charged PNGBs, to that of the extra scalars in "two-Higgs" models. Therefore, in this work, we will largely be concerned with the properties of colored resonances and PNGBs. These models have a possibly unique signature: resonances associated with the *electroweak* symmetry breaking sector which are *strongly produced*. Hadron colliders will be especially important for searching for signatures of such colored particles associated with EWSB.

# 2   A Field Guide to Models

In this section we survey models with a dynamical EWSB sector, and summarize some of the novel physics that may be necessary in a model consistent with present data. We do not consider any of the models discussed in this section to be a complete theory of EWSB — in fact most of these models are ruled out by one or more of the problems listed below. Their main value lies in illustrating some of the possible physics which may appear in a complete dynamical theory of EWSB.

Models incorporating ETC interactions ran into trouble with flavor changing neutral currents (FCNCs) [7, 8] in the early 1980's. For example, models with flavor dependent ETC gauge couplings generically produce four-fermion interactions like:

$$\mathcal{L}_{4f} = \frac{g_{ETC}^2 c_\theta^2 s_\theta^2}{2M_{ETC}^2} \left(\overline{s}_L \gamma_\mu d_L\right) \left(\overline{s}_L \gamma^\mu d_L\right) \ , \tag{1}$$

where $c_\theta$ and $s_\theta$ are the cosine and sine of a model-dependent mixing angle; and $M_{ETC}$ and $g_{ETC}$ are the ETC gauge boson mass and coupling respectively. The interaction in equation (1) contributes to the $K_L - K_S$ mass splitting, and in order that this contribution be smaller than the short-distance, standard model contribution, we must have (taking the mixing angle to be equal to the Cabibbo angle):

$$\frac{M_{ETC}}{g_{ETC}} > 200 \, \text{TeV} \ . \tag{2}$$

On the other hand, the mass of an ordinary fermion is expected to be given by

$$m_f \approx \frac{g_{ETC}^2 < \overline{\Psi}\Psi >}{M_{ETC}^2} \ , \tag{3}$$

where $\Psi$ is the technifermion field [6, 7]. If we assume that the TC dynamics is QCD-like, we can estimate the technifermion condensate by scaling from QCD [9]:

$$< \overline{\Psi}\Psi > \approx 4\pi F^3 \ . \tag{4}$$

Given that $F$ cannot be larger[1] than 246 GeV, it is impossible to generate a large enough mass for the $s$ quark (much less the $c$ quark) using the above relations.

Two possible solutions to the conflict between large fermion masses and small FCNCs were proposed in the mid and late 1980's. The first solution was to make the TC gauge coupling run slower than in QCD (this behavior was dubbed walking) [10]. This has the effect of making the technifermion condensate much larger than scaling from QCD suggests, so that for a fixed quark or lepton mass, the necessary mass scale for ETC gauge bosons is increased, thus suppressing FCNCs. The

---

[1]Having more than one doublet, or having technifermions in higher representations of $SU(2)_L$, reduces the value of $F$ needed to generate the correct $W$ mass.

second solution was to build a Glashow-Illiopoulos-Maiani (GIM) [11] symmetry into the ETC theory (this is sometimes called TechniGIM) [12, 30, 40]. This mechanism allows for ETC scales as low as 1 TeV.

A further problem is how to produce a large isospin splitting for the $t$ and $b$ quark masses without producing large isospin splitting in the $W$ and $Z$ masses [13]. Isospin splitting in the gauge sector is described by the radiative correction parameter $T$ (a.k.a. $\Delta\rho_*$), which is tightly constrained by experimental data.

A completely different alternative for model building is to include a scalar that couples to both fermions and technifermions in the model [32]. This has the advantage that it allows for a standard GIM symmetry, and can produce acceptable isospin splitting. The scalar may be kept light by supersymmetry [36], or it may be a composite, formed by some strong (fine-tuned) four-fermion interaction, for example [14]. The latter possibility arises in models with strong ETC interactions [15], which can be a natural result of walking, since walking implies that the TC coupling remains large out to the scale where TC is embedded in ETC. Scalars or strong ETC interactions are also helpful in producing large top quark masses.

A further twist on the TC scenario goes under the rubric of multiscale models [16]. The original idea was that technifermions in different representations of the TC gauge group should condense at different scales, thus producing more than one scale of EWSB. (Higher dimension TC representations may be useful for producing walking couplings.) Multiple EWSB scales can also be produced in other ways. For example in walking and/or strong ETC models, the effects of QCD interactions can produce a large splitting between techniquarks and technileptons [17].

An additional challenge for TC models was noticed more recently [18]: models with QCD-like dynamics tend to produce large positive contributions to the electroweak radiative correction parameter $S$ which grow with the number of technicolors and the number of technidoublets, while experiments tend to prefer small values for $S$. There are several possibilities for evading this problem. There may simply be very few technifermions which contribute to EWSB, so that the contribution to $S$ is small. Alternatively, mechanisms can be invented which produce a negative contribution to $S$: the technifermions may have exotic electroweak quantum numbers [19], or the TC dynamics can be sufficiently unlike QCD so as to invalidate the naive scaling-up of QCD phenomenology [20, 21, 37]. Both of these alternatives usually also rely on some form of isospin breaking. This makes multi-scale models potentially very useful since the bulk of the isospin breaking necessary to produce a negative contribution to $S$ can occur in the lowest EWSB scale [21], whereas the $T$ parameter is sensitive to isospin breaking at the highest EWSB scale.

The most recent problem for ETC models arises from the measurement of the $Z \rightarrow b\bar{b}$ partial width at LEP [22, 43]. The experiments find a partial width which is slightly larger than the standard model prediction, while almost all the ETC models that have been constructed so far produce a correction which further re-

duces this width. The sign of the correction is a consequence of the almost universal assumption that $SU(2)_L$ commutes with the ETC gauge group. The alternative, where $SU(2)_L$ is embedded in the ETC gauge group, may be interesting, since this reverses the sign of the correction [43]. (Models with scalars and/or strong ETC, can make the ETC correction unobservably small [23].)

Table 1: Field guide to models summary table. The abbreviated headings are: the number of technicolors ($N_{tc}$), the dimension of the representation which condenses to break the electroweak gauge symmetry ($d$), the number of doublets ($N_d$), the pattern of electroweak symmetry breaking [48], the presence of a walking technicolor coupling, scalars and/or strong ETC (SETC), multiscale (MS), GIM suppression of flavor changing neutral currents, or non-commuting (NC) ETC and weak gauge groups.

| ref. | $N_{tc}$ | $d$ | $N_d$ | pattern | walking | SETC | MS | GIM | NC |
|------|----------|-----|-------|---------|---------|------|----|-----|-----|
| 24 | 4 | 5 | 12 | $O$ | | | $\checkmark$ | | |
| 25 | 6 | 6 | 4 | $O$ | | | | | |
| 26 | 2 | 4 | 4 | $Sp$ | $\checkmark$ | $\checkmark$ | | $\checkmark$ | |
| 27 | 5 | 5 | >3 | $O$ | | | | | |
| 28 | 3 | 3 | 7 | $SU$ | | | | | |
| 29 | $N$ | $N$ | >3 | $SU$ | | | | | |
| 30 | $N$ | $N$ | >3 | $SU$ | | | | $\checkmark$ | |
| 31 | 4 | 4 | 1 | $SU$ | | $\checkmark$ | | $\checkmark$ | |
| 32 | $N$ | $N$ | 1 | $SU$ | | $\checkmark$ | | $\checkmark$ | |
| 33 | 6 | 6 | 1 | $SU$ | | $\checkmark$ | | $\checkmark$ | |
| 34 | 7 | 7 | 4 | $O$ | | | | | |
| 35 | 2 | 2 | 8 | $Sp$ | $\checkmark$ | | | | |
| 36 | $N$ | $N$ | 1 | $SU$ | | $\checkmark$ | | $\checkmark$ | |
| 37 | 6 | 15 | 10 | $SU$ | $\checkmark$ | | $\checkmark$ | | |
| 38 | 4 | 5 | 12 | $O$ | $\checkmark$ | | $\checkmark$ | | |
| 39 | 2 | 2 | 1 | $Sp$ | $\checkmark$ | $\checkmark$ | | | |
| 40 | $N$ | $N$ | 1 | $SU$ | | | | $\checkmark$ | |
| 41 | 2 | 1 | 8 | $SU$ | $\checkmark$ | $\checkmark$ | $\checkmark$ | | |
| 42 | 2 | 2 | 4 | $Sp$ | $\checkmark$ | $\checkmark$ | $\checkmark$ | | |
| 43 | $N$ | $N$ | >3 | $SU$ | | | $\checkmark$ | | $\checkmark$ |

Some of the ideas mentioned here rely heavily on non-QCD-like dynamics (i.e. walking, composite scalars, strong ETC, multiple scales). The flip-side of relying on non-QCD-like models is that the more unlike QCD the dynamics is, the more unreliable the calculation is. This brings us face-to-face with the central problem of building models for strong EWSB: writing down a model Lagrangian is not enough, since there are strong interactions involved, at present we usually have to

guess at the qualitative features of the model.

In order to summarize the status of model building, we have produced Table 1. Of course we cannot hope to present the intricacies of these models in tabular form. For models with more than one type of TC representation, the number of doublets shown is only approximate. The table is not complete, but it is hopefully representative, and provides a quick overview of the types of models which have been (at least partially) explored.

# 3    Particle Spectrum, Masses and Couplings

## 3.1    Particle spectrum and gauge quantum numbers

In non-minimal technicolor models one expects that the presence of colored techni-fermions will result in a spectrum of PNGBs ($P$'s) and vector resonances ($\rho_T$'s and $\omega_T$), some of which may carry color quantum numbers. These particles may be classified by their $SU(3)_C$ and $SU(2)_V$ quantum numbers as shown in Table 2. Hereafter we will follow the nomenclature defined in EHLQ [44].

Table 2: Spectrum of particles in non-minimal technicolor models.

| $SU(3)_C$ | $SU(2)_V$ | Particle |
|---|---|---|
| 1 | 1 | $P^{0\prime}$ , $\omega_T$ |
| 1 | 3 | $P^{0,\pm}$ , $\rho_T^{0,\pm}$ |
| 3 | 1 | $P_3^{0\prime}$ , $\rho_{T3}^{0\prime}$ |
| 3 | 3 | $P_3^{0,\pm}$ , $\rho_{T3}^{0,\pm}$ |
| 8 | 1 | $P_8^{0\prime}(\eta_T)$ , $\rho_{T8}^{0\prime}$ |
| 8 | 3 | $P_8^{0,\pm}$ , $\rho_{T8}^{0,\pm}$ |

The minimal technicolor model [3] includes the three Nambu-Goldstone bosons that give rise to the longitudinal components of the weak gauge bosons and the color neutral $\rho_T$ and $\omega_T$ [45]. Since we will pursue physics beyond the minimal model we will focus on the extra color-neutral PNGBs and the colored particles, excepting the color triplets $(P_3, \rho_{T3})$ which have the same phenomenology as leptoquarks and, as such, will be studied in ref. 46 in the case where the leptoquarks decay predominantly in the first and second generation fermions.

## 3.2    Masses

We consider here the three main contributions to the masses of the particles listed in Table 2: strong TC interactions, QCD interactions, and ETC interactions. In

the limit where standard model interactions and ETC interactions are turned off, the PNGBs would be massless and the techni-vector-mesons ($\rho_T$ and $\omega_T$) would have masses set by the scale(s) of the TC interaction. Given the possibility of multiscale models (as discussed in section 2), these masses could conceivably range from 100 GeV to 2 TeV.

Turning on QCD interactions causes the color octet PNGBs to receive mass contributions from graphs with a single gluon exchange. The calculation of the PNGB masses parallels that of the $\pi^+$-$\pi^0$ mass splitting in QCD [47, 48]. Recall that to leading order in the fine structure constant:

$$m_{\pi^+}^2 - m_{\pi^0}^2 = \alpha M_{QCD}^2 \; . \tag{5}$$

where $M_{QCD}$ is a strong interaction parameter that must be taken from experiment. The analogous result for the octet PNGBs ($P_8^{0,\pm,\prime}$) is [48]:

$$m_{P_8}^2|_{QCD} = 3\alpha_s M_{TC}^2 \; . \tag{6}$$

For $SU(N)$ TC models with QCD-like dynamics we can estimate the parameter $M_{TC}$ by scaling up QCD and using large $N$ arguments, which gives [48]:

$$M_{TC} \approx \frac{8\,F}{\sqrt{N}} \; , \tag{7}$$

where $F$ is the TC analog of $f_\pi$. Equations (6) and (7) suggest mass contributions for octet PNGBs in the range 200-400 GeV. There is a similar contribution to the masses of color triplet PNGBs [48], with the 3 in equation (6) replaced by 4/3. We expect additional uncertainties for models (multiscale, walking, strong ETC) where the TC dynamics is quite different from QCD.

Finally, turning on the ETC interactions can give rise to masses for the color singlet PNGBs. Although the ETC contributions to the PNGB masses are entirely model dependent, we expect, based on Dashen's formula [49], that these contributions have the following form:

$$m_P^2|_{ETC} \approx \frac{<\overline{\Psi}\Psi\overline{\Psi}\Psi>}{F^2\Lambda_f^2} \; , \tag{8}$$

where $\Psi$ is the technifermion field, and $\Lambda_f \equiv M_{ETC}/g_{ETC}$ is the ETC scale associated with an ordinary fermion $f$. Assuming that the vev of the four-fermion operator factorizes, we have:

$$m_P|_{ETC} \approx \frac{<\overline{\Psi}\Psi>}{F\Lambda_f} \; . \tag{9}$$

Recalling that the standard estimate of an ordinary fermion mass is:

$$m_f \approx \frac{<\overline{\Psi}\Psi>}{\Lambda_f^2} \; , \tag{10}$$

we can write

$$m_P|_{ETC} \approx \frac{m_f}{F} \Lambda_f \ . \tag{11}$$

If there exists a consistent dynamical model of EWSB which can produce a heavy enough $t$ quark, then using a $t$ quark mass of 170 GeV, $F$ of 123 GeV, and an ETC scale at least as large as the technicolor scale of a TeV, we have a contribution to the PNGB mass of the order of a TeV! Alternatively using the $c$ ($s$) quark, and an ETC scale of 100 TeV (necessary in order to suppress FCNCs) we have a contribution of 1.2 TeV (136 GeV). Thus it may not be surprising if PNGBs are not found at colliders any time soon.

## 3.3 Gauge couplings

The gauge couplings of the PNGBs and vector resonances are determined by their quantum numbers. The relevant vertices are summarized in Tables 3 and 4.

Table 3: Three and four-point electroweak gauge couplings.

| | $\gamma_\mu[Z_\mu]$ | $\gamma_\mu\gamma_\nu$ |
|---|---|---|
| $P^+P^-$ | $-ie[\frac{e(1-2\sin^2\theta_w)}{2\sin\theta_w\cos\theta_w}](p_+ - p_-)_\mu$ | $2ie^2 g_{\mu\nu}$ |
| $P_{8a}^+ P_{8b}^-$ | $-ie[\frac{e(1-2\sin^2\theta_w)}{2\sin\theta_w\cos\theta_w}](p_+ - p_-)_\mu \delta_{ab}$ | $2ie^2 g_{\mu\nu}\delta_{ab}$ |
| $\rho_{8Ta\alpha}^+ \rho_{8Tb\beta}^-$ | $ie[\frac{e}{\tan\theta_w}]((p_+ - p_-)_\mu g_{\alpha\beta} + p_{-\alpha} g_{\beta\mu} - p_{+\beta} g_{\alpha\mu})\delta_{ab}$ | $ie^2(g_{\alpha\nu}g_{\beta\mu} + g_{\beta\nu}g_{\alpha\mu} - 2g_{\alpha\beta}g_{\mu\nu})\delta_{ab}$ |

Table 4: Three and four-point QCD gauge couplings.

| | $g_{c\mu}$ | $g_{c\mu}g_{d\nu}$ |
|---|---|---|
| $P_{8a}^{+,0,\prime} P_{8b}^{-,0,\prime}$ | $-gf_{abc}(p_a - p_b)_\mu$ | $ig^2(f_{ace}f_{bde} + f_{ade}f_{bce})g_{\mu\nu}$ |
| $\rho_{8Ta\alpha}^{+,0,\prime} \rho_{8Tb\beta}^{-,0,\prime}$ | $-gf_{abc}((p_a-p_b)_\mu g_{\alpha\beta} - p_{a\beta}g_{\alpha\mu} + p_{b\alpha}g_{\beta\mu})$ | $ig^2((f_{ace}f_{bde} + f_{ade}f_{bce})g_{\mu\nu}g_{\alpha\beta} - f_{ace}f_{bde}g_{\nu\alpha}g_{\mu\beta} - f_{ade}f_{bce}g_{\mu\alpha}g_{\nu\beta})$ |

## 3.4 Strong couplings

Here we assume that we can scale the strong coupling obtained from $\rho \to \pi\pi$ in QCD to estimate the strong coupling between $\rho_T$'s and $P$'s in a technicolor model:

$$\alpha_{\rho_T} = \frac{g_{\rho_T}^2}{4\pi} = 2.97 \left[\frac{3}{N}\right] \tag{12}$$

where $N$ specifies the technicolor group $\text{SU}(N)_{TC}$. It is not clear how this result would change in a non-QCD-like technicolor model. The relevant vertices are given in Table 5 below.

Table 5: Vector-PNGB-PNGB strong coupling.

| | |
|---|---|
| $\rho_{8Ta\mu}P_{8b}P_{8c}$ | $-\frac{1}{\sqrt{2}}\,g_{\rho_T}f_{abc}(p_b - p_c)_\mu$ |
| $\rho_{8Ta\mu}^{\pm 0}P_{8b}^{0\pm}P^{\mp}$ | $-\frac{1}{2\sqrt{3}}\,g_{\rho_T}(p_b - p)_\mu\delta_{ab}$ |

## 3.5   Vector-meson dominance and mixing

The color-octet, isospin singlet technirho has the same quantum numbers as a gluon. Hence these states can in principle mix in the same way that the rho and the photon mix under the usual strong interactions. Assuming a generalization of vector meson dominance for the gluon-$P_8$-$P_8$ interaction, the technirho-gluon mixing constant is given by:

$$g_{\rho_T-g} = \frac{\sqrt{2}\,g_s M_{\rho_T}^2}{g_{\rho_T}} \tag{13}$$

This coupling will be important for single $\rho_{8T}^{0\prime}$ production at hadron colliders.

## 3.6   Flavor dependent couplings

The coupling of technipions to ordinary fermions are induced by ETC interactions and hence are model dependent. However, these couplings are generally proportional to the fermion masses. We assume that the coupling of the neutral technipions is flavor diagonal in order to avoid FCNC and we parameterize these couplings in Table 6 [52].

ETC interactions also induce a direct coupling between vector resonances and fermions which can be characterized by [51] :

$$\mathcal{A}_{ETC}(\rho_T \to f\bar{f}) = \frac{g_{ETC}^2}{M_{ETC}^2}\frac{M_{\rho_T}^2}{g_{\rho_T}}\bar{f}\gamma_\mu f\epsilon^\mu \tag{14}$$

These interactions are also flavor dependent since the ETC coupling constant $g_{ETC}$ is related to quark masses and hence is strongest for the top and bottom quarks. Assuming that these interactions generate the top quark mass one can estimate :

$$\frac{g_{ETC}^2}{M_{ETC}^2} \simeq \frac{m_t}{4\pi F^3} \tag{15}$$

9

Table 6: Order of magnitude of the couplings of technipions to ordinary fermions, where $V_{ff'}$ is a model dependent mixing matrix.

| $P^{0,\prime} f \bar{f}$ | $\frac{m_f}{F} \bar{f} \gamma_5 f$ |
|---|---|
| $P_{8a}^{0,\prime} f \bar{f}$ | $\frac{m_f}{F} \bar{f} \frac{\lambda_a}{2} \gamma_5 f$ |
| $P^{\pm} f \bar{f'}$ | $\frac{m_f}{F} \bar{f} \gamma_5 f V_{ff'}$ |
| $P_{8a}^{\pm} f \bar{f}$ | $\frac{m_f}{F} \bar{f} \frac{\lambda_a}{2} \gamma_5 f V_{ff'}$ |

## 3.7  Anomalous couplings

The low energy coupling of a PNGB to a pair of gauge fields $B_1, B_2$ is dominated by the ABJ anomaly [68] because of the relation of the PNGB to the axial current via PCAC. The coupling can be written as [50] :

$$\frac{S_{PB_1B_2}}{8\sqrt{2}\pi^2 F} \varepsilon_{\mu\nu\alpha\beta} \epsilon_1^\mu \epsilon_2^\nu k_1^\alpha k_2^\beta \qquad (16)$$

where $k$ and $\epsilon$ are the momentum and polarization 4-vectors of the gauge bosons and the anomaly factors $S_{PB_1B_2}$ are model dependent. For the one-family $SU(N)_{TC}$ model with $F = 123$ GeV the anomaly factors are listed in Table 7.

Other anomalous couplings involve the vector resonances and are the analogues of the couplings allowing for $\rho(\omega) \to \pi\gamma$ processes in QCD. They can be parameterized as shown in Table 8 [51].

Table 7: PNGB anomalous couplings.

| Vertex | Anomaly factor S |
|---|---|
| $P^0\gamma\gamma$ | $e^2 4N/\sqrt{6}$ |
| $P^0\gamma Z$ | $e^2 2N/\sqrt{6}\left(\frac{1-4\sin^2\theta_W}{\sin 2\theta_W}\right)$ |
| $P^0 ZZ$ | $-e^2 N/\sqrt{6}\left(\frac{2-4\sin^2\theta_W}{\cos^2\theta_W}\right)$ |
| $P^0 W^+ W^-$ | $0$ |
| $P^{0\prime}\gamma\gamma$ | $-e^2(4N/3\sqrt{6})$ |
| $P^{0\prime}\gamma Z$ | $e^2(4N/3\sqrt{6})\tan\theta_W$ |
| $P^{0\prime}ZZ$ | $-e^2(4N/3\sqrt{6})\tan^2\theta_W$ |
| $P^{0\prime}W^+ W^-$ | $0$ |
| $P^{0\prime}g_a g_b$ | $g_s^2 N/\sqrt{6}\delta_{ab}$ |
| $P^0_{8a}g_b\gamma$ | $g_s eN\delta_{ab}$ |
| $P^0_{8a}g_b Z$ | $g_s eN\frac{1-\sin^2\theta_W}{\sin 2\theta_W}\delta_{ab}$ |
| $P^{0\prime}_{8a}g_b g_c$ | $g_s^2 N d_{abc}$ |
| $P^{0\prime}_{8a}g_b\gamma$ | $g_s eN/3\delta_{ab}$ |
| $P^{0\prime}_{8a}g_b Z$ | $-g_s eN/3\tan\theta_W\delta_{ab}$ |
| $P^{\pm}\gamma W^{\mp}$ | $e^2 N/(\sqrt{6}\sin\theta_W)$ |
| $P^{\pm}ZW^{\mp}$ | $-e^2 N/(\sqrt{6}\cos\theta_W)$ |
| $P^{\pm}_{8a}g_b W^{\mp}$ | $g_s eN/(2\sin\theta_W)\delta_{ab}$ |

Table 8: Vector resonances anomalous couplings.

| | |
|---|---|
| $\rho^{\pm,0,0\prime}_{8Ta\mu}P^{\mp,0,0\prime}_{8b}\gamma_\nu(Z_\nu)$ | $ie\frac{\kappa_{\gamma(Z)}}{F}\varepsilon_{\mu\nu\alpha\beta}p^\alpha_P p^\beta_{\gamma(Z)}\delta_{ab}$ |
| $\rho^{\pm,0,0\prime}_{8Ta\mu}P^{\mp,0,0\prime}_{8b}g_{\nu c}$ | $ig_s\frac{\kappa_g}{F}\varepsilon_{\mu\nu\alpha\beta}p^\alpha_P p^\beta_g f_{abc}$ |
| $\rho^{\pm,0,0\prime}_{8Ta\mu}P^{\mp,0,0\prime}g_{\nu b}$ | $ig_s\frac{\kappa_g}{F}\varepsilon_{\mu\nu\alpha\beta}p^\alpha_P p^\beta_g\delta_{ab}$ |

# 4  Production Rates and Signatures in Hadron Colliders

## 4.1  PNGB single production

We use the narrow width approximation to write a differential cross section for partons $a$ and $b$ to produce a single resonance $A$ as:

$$\frac{d\sigma(pp \to A + X)}{dy} = \frac{32\pi^2}{s} \sum_{a,b} C_{ab} \frac{(2S_A + 1)}{(2S_a + 1)(2S_b + 1)} \frac{\Gamma(A \to ab)}{m_A} \left[ f_{a/p}(\sqrt{\tau}e^y) f_{b/p}(\sqrt{\tau}e^{-y}) \right]$$

(17)

where the color factor is $C_{gg} = 1/64$ or $C_{q\bar{q}} = 1/9$, $y$ is the rapidity of the $ab$ system in the $pp$ center-of-mass frame and $f_{a/p}$ is the parton $a$ distribution function inside a proton, and $\tau = m_A^2/s$.

The widths relevant for production and decay of $P^{0\prime}$ and $P_8^{0\prime}$ in the one-family model are :

$$\Gamma(P^{0\prime} \to l\bar{l}(q\bar{q})) = \frac{(3)}{8\pi} \frac{m_{l(q)}^2}{F^2} m_P \left(1 - 4m_{l(q)}^2/m_P^2\right)^{3/2} \tag{18}$$

$$\Gamma(P_8^{0\prime} \to q\bar{q}) = \frac{3}{16\pi} \frac{m_q^2}{F^2} m_P \left(1 - 4m_q^2/m_P^2\right)^{3/2} \tag{19}$$

$$\Gamma(P^{0\prime} \to gg) = \frac{\alpha_s^2}{6\pi^3} \left(\frac{N}{4}\right)^2 \frac{m_P^3}{F^2} \tag{20}$$

$$\Gamma(P^{0\prime} \to \gamma\gamma) = \frac{\alpha^2}{27\pi^3} \left(\frac{N}{4}\right)^2 \frac{m_P^3}{F^2} \tag{21}$$

$$\Gamma(P_8^{0\prime} \to gg) = \frac{5\alpha_s^2}{24\pi^3} \left(\frac{N}{4}\right)^2 \frac{m_P^3}{F^2} \tag{22}$$

$$\Gamma(P_8^{0\prime} \to gZ) = \frac{\alpha\alpha_s}{144\pi^3} \left(\frac{N}{4}\right)^2 \tan^2\theta_W \frac{m_P^3}{F^2} \,. \tag{23}$$

The rate of $P_8^{0\prime}$ production is illustrated in Figure 1. In Figure 2 we show the various decays widths of the $P_8^{0\prime}$ in the one-family model.

Even though the PNGBs are copiously produced, they predominantly decay into two (gluon or b-quark) jets and the signal is completely swamped by the QCD background. If the PNGB mass is above the $t\bar{t}$ threshold, the decay mode $P \to t\bar{t}$ becomes dominant and may alter the standard QCD value of the $t\bar{t}$ cross section. This signature will be separately discussed below. The rare decay mode $P_8^{0\prime} \to Zg$ is interesting and is under study [53] to see whether it is visible above the background from $pp \to ZgX$.

For $m_P < m_t/2$, the best hope of finding $P^{0\prime}$ at a hadron collider is through the rare decay modes $P^{0\prime} \to \gamma\gamma$ and $P^{0\prime} \to \tau^+\tau^-$. The signal in the two-photon channel
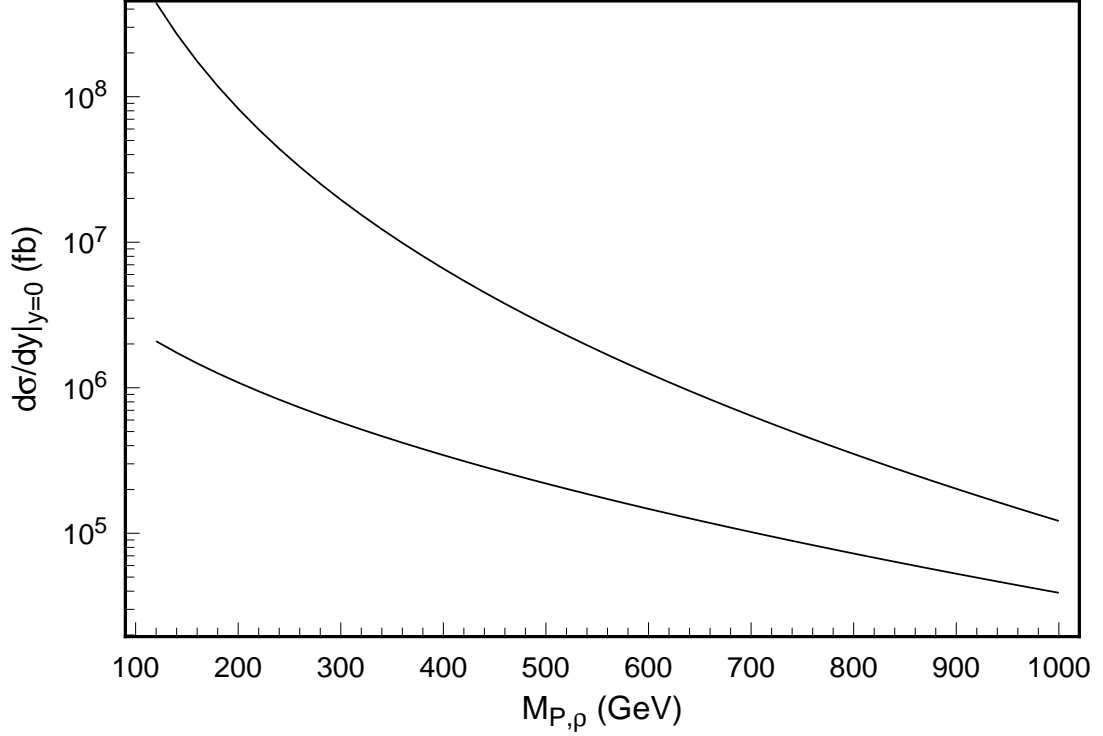
Figure 1: Differential cross section at $y = 0$ for single production of $\rho_{T8}^{0\prime}$ (solid line) and $P_8^{0\prime}$ (dashed line) at the LHC in femtobarns.

would resemble that of an intermediate mass Higgs boson; the small branching ratio (of order 0.001) is compensated by the large production rate. The signal in the $\tau^+\tau^-$ final state has as background the corresponding Drell-Yan process. According to ref. 44 the *effective* integrated luminosity (i.e. luminosity times identification efficiency) required to find the $P^{0\prime}$ in this channel would be in the range $3 \times 10^{35}$ $- 5 \times 10^{36} \mathrm{cm}^{-2}$ for colliders with center-of-mass energies in the range $2 - 20$ TeV.
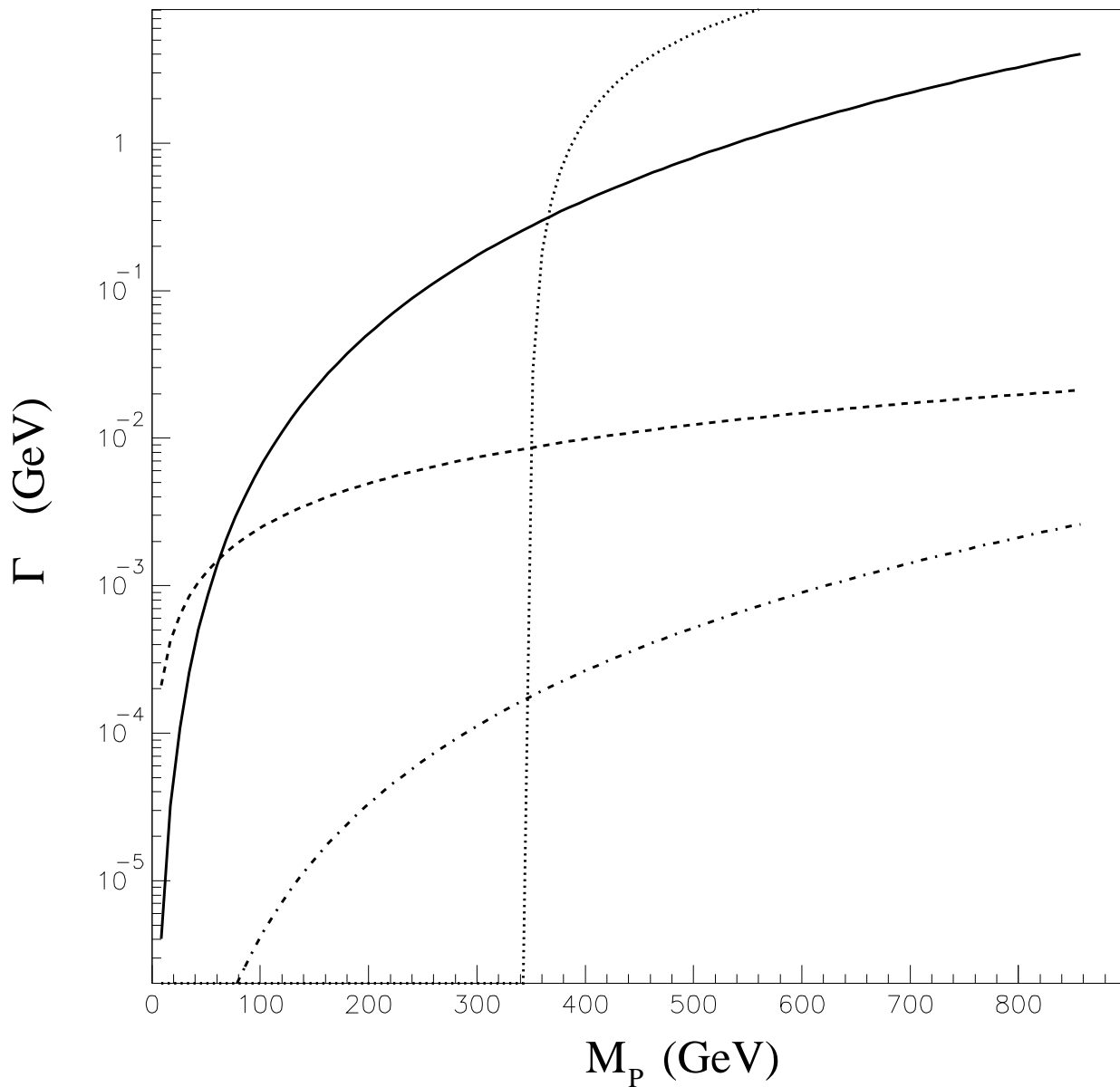
Figure 2: Partial widths for the decay of $P_8^{0\prime}$ into gluon-gluon (solid line), $\bar{b}b$ (dashed line), $\bar{t}t$ (dotted line) and $Z$-gluon (dot-dashed line) in the one-family model.

14

## 4.2   PNGB pair production

The large color charge of the color-octet PNGBs produces two phenomenological advantages. It allows them to be copiously produced at hadron colliders (see Table 9) and it enables them to decay hadronically to two jets[2]. The net result can be spectacular four-jet signals of a strongly-interacting electroweak symmetry breaking sector. That is, one can potentially identify this new physics in multi-jet final states without recourse to charged-lepton or missing-energy triggers. Evaluating the ability of a given collider to find new colored particles in multi-jet final states involves estimating the QCD multi-jet background, calculating the signal from heavy particle decays, and choosing kinematic variables in which the signal stands out cleanly above background. Such estimates have been made [54, 55] for several types of new colored particles at both the LHC and the Tevatron.

Table 9:   Production cross-sections for color-octet scalars as a function of mass at the Tevatron and LHC.

| $M_P$ $(GeV)$ | Collider | $\sigma_{scalar}(pb)$ |
|---|---|---|
| 25 | TeV | 85.0 |
|    | LHC | — |
| 50 | TeV | 0.0897 |
|    | LHC | 217. |
| 100 | TeV | 85.0 |
|     | LHC | 11,900 |
| 250 | TeV | 0.0897 |
|     | LHC | 217. |
| 500 | TeV | — |
|     | LHC | 6.34 |

The QCD background for multi-jet processes can be estimated by starting with the results of Parke and Taylor [56] for the cross-section for the maximally-helicity-violating $gg \rightarrow gggg$ processes, assuming [54] that all non-zero helicity amplitudes contribute equally, and employing the effective structure function approximation $F(x_i) = g(x_i) + \frac{4}{9}[q(x_i) + \bar{q}(x_i)]$. These approximations have been found [57] to agree with exact results within the intrinsic error due to neglecting higher-order corrections and to imperfect knowledge of $\alpha_s$, $q^2$ and the structure functions. In order to insure that the jets will be separately detectable, it is necessary to require that they be central and well-separated.

---

[2]By two jets, we mean either a light quark anti-quark pair or two gluons; a PNGB decaying preferentially to a $t\bar{t}$ pair would have a very different signature.

15

Signal events are those arising from pair-production and two-jet decays of colored PNGBs. The production cross section [44] for a real colored scalar $(P)$ in the D-dimensional representation of $SU(3)_{color}$ is

$$\frac{d\sigma}{d\hat{t}}(q\bar{q} \to PP) = \frac{\pi\alpha_s^2}{9\hat{s}^2}k_D\beta^2(1-z^2),\qquad(24)$$

for quark anti-quark annihilation and

$$\frac{d\sigma}{d\hat{t}}(gg \to PP) = \frac{\pi\alpha_s^2 k_D}{\hat{s}^2}\left(\frac{k_D}{D} - \frac{3}{32}(1-\beta^2 z^2)\right)(1-2V+2V^2),\qquad(25)$$

for gluon fusion. Here $z = \cos\theta^*$ measures the partonic c.m. scattering angle, $\hat{s}$ is the partonic c.m. energy squared, $k_D$ is the Dynkin index of the D-dimensional $SU(3)_{color}$ representation $(k_8 = 3)$,

$$V = 1 - \frac{1-\beta^2}{1-\beta^2 z^2},\qquad(26)$$

and

$$\beta^2 = 1 - 4m_P^2/\hat{s},\qquad(27)$$

where $m_P$ is the mass of the scalar. As stated above, the PNGBs are assumed to decay to two jets, resulting in four-jet events. In order to insure that the decay jets will be detectable, one must require them to be central and well-separated using the same cuts applied to the QCD background

Even for central, well-separated jets, the QCD background is large enough that some care must be used in choosing the kinematic variables in which to search for the signal. For instance, the enhancement in $d\sigma/d\sqrt{(\hat{s})}$ above the new particle's pair-production threshold is too small to be detectable. However, the following strategy brings out the signal: Given a four-jet event, consider all possible partitions of the jets into two clusters of two jets each. Choose the partition with the two clusters closest in squared invariant mass, and define the "balanced cluster mass" $m_{bal}$ as the average of the cluster masses. Then if the cross-section is considered as a function of $m_{bal}$, the signal will cluster about $m_{bal} = m_{new\ particle}$ while the background will not. The signal can be further enhanced by imposing a relatively large minimum-$p_T$ cut on the jets; the background is strongly peaked at low $p_T$ due to the infrared singularities of QCD and the signal is not. An illustration of this method is shown in Figure 3 below. Analyses of this kind indicate that real scalar color-octet particles of a mass as high as 325 GeV should be visible at the LHC if a $p_T$ cut of about 170 GeV is employed[3]. The lower end of the visible mass range depends strongly on just how energetic $(p_T^{min})$ and well-separated $(\Delta R)$ jets must be in order for an event to be identified as containing four distinct jets. Discovery

---

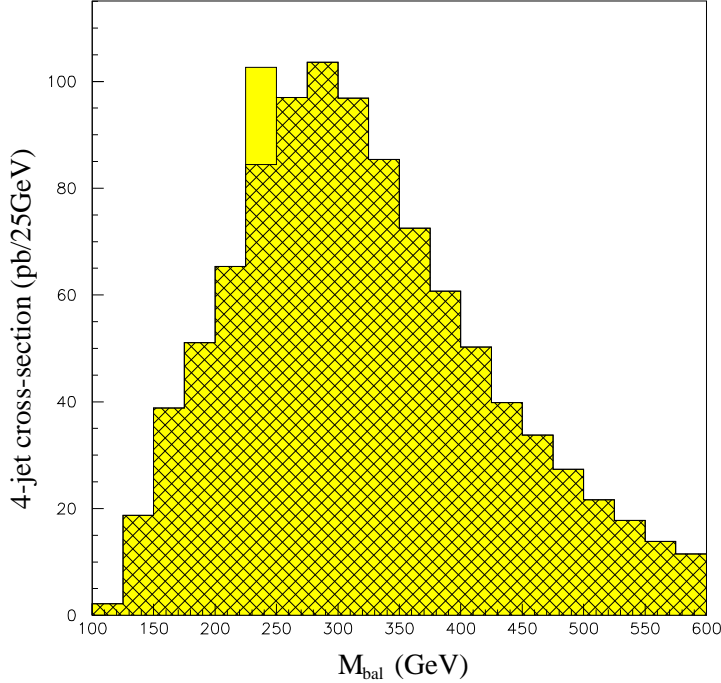[3]This is derived by scaling from the result in ref. 55.

Figure 3: Four-jet rate $\frac{d\sigma}{dm_{bal}}$ at a 17 TeV collider with $p_T^{min}$ of 100 GeV. QCD background (hatched) and 240 GeV technipion signal are shown. No resolution effects included. Taken from ref. 52.

of color-octet scalars at the Tevatron is likely to be difficult; it is estimated that those potentially accessible at the Tevatron are so light (of order 10-20 GeV) that they would already have been seen at LEP if they carried electroweak quantum numbers [55].

## 4.3 Vector resonance production

Once again we employ the narrow width approximation and the production cross section of equation 17. The $\rho_{T8}^{0\prime}$ can always decay to either $gg$ or $q\bar{q}$ via its mixing with the gluon using the assumption of a generalized vector meson dominance. Hence the partial widths relevant for $\rho_{T8}^{0\prime}$ production are given by :

$$\Gamma(\rho_{T8}^{0\prime} \to gg) = \frac{\alpha_s^2}{2\alpha_\rho} m_\rho \qquad (28)$$

17

$$\Gamma(\rho_{T8}^{0\prime} \to q\bar{q}) \;\; = \;\; \frac{5\alpha_s^2}{6\alpha_\rho} m_\rho \tag{29}$$

In Figure 1 we compare the single production cross section of the $\rho_{T8}^{0\prime}$ and $P_8^{0\prime}$ at the LHC.

While the widths (28) and (29) are important for $\rho_{T8}^{0\prime}$ *production*, if kinematically allowed the dominant decay mode is into two colored PNGB:

$$\Gamma(\rho_{8T}^{0\prime} \to P_8 P_8) = \frac{\alpha_{\rho_T}}{4} \, m_\rho \, \left(1 - 4m_P^2/m_\rho^2\right)^{3/2}. \tag{30}$$

In this case the $\rho_{T8}^{0\prime}$ contributes strongly to the cross section for color-octet PNGB pair production discussed in the previous subsection and improves the signal.

In models where the above decay is not kinematically accessible, the $\rho_{T8}^{0\prime}$ is very narrow ($\Gamma \simeq 4$ GeV) and it decays primarily into dijets. The authors of ref. 37 conclude that, "up to questions of resolution, acceptance and background" the $\rho_{T8}^{0\prime}$ may be observable at the Tevatron for $M_{\rho_{T8}^{0\prime}} \sim 200$–600 GeV. A preliminary analyses from CDF indicates that a $\rho_{T8}^{0\prime}$ with mass in the range $260 < M_{\rho_{T8}^{0\prime}} < 470$ GeV has been excluded at 95% confidence level [58].

If the $\rho_{T8}$ are light, as in multiscale models, then one would have a sizeable cross section for their *pair* production. Naïvely, well above threshold for pair production of vector resonances, one would expect :

$$\frac{\sigma(pp \to \rho_{T8} + X)}{\sigma(pp \to \rho_{T8}\rho_{T8} + X)} \simeq \frac{1}{g_{\rho_T}^2} \simeq \frac{1}{40}. \tag{31}$$

Furthermore, one can pair produce *all* types of colored vector resonances, whereas in the single production via gluon mixing the isosinglet $\rho_{8T}^{0\prime}$ is dominant. This may result in interesting decays to longitudinal electroweak gauge bosons, that would not be shared by the single-production mechanism. One may also expect spectacular 8–jet events that could be extracted from the generic QCD background due to their peculiar kinematics, just as in the case of color-octet PNGB pair production. To our knowledge, this has not been studied in the literature.

## 4.4  Colored PNGBs and Gauge Boson Pairs

If the electroweak symmetry breaking sector contains colored technipions, then as shown in sections 4.1 and 4.2 they can be copiously produced at a high-energy hadron collider. In addition to detecting the technipions directly, one can detect them after they have re-scattered into pairs of $W$ or $Z$ particles. For example, in the one-family technicolor model $P_8^{0,\pm} P_8^{0,\pm} \to WW$ or $ZZ$. Therefore, in these models the production of gauge boson pairs through gluon fusion includes a contribution from loops of colored technipions. As suggested by Bagger, Dawson, and Valencia

[59], this mechanism can lead to a significant enhancement in the number of gauge-boson pairs observed at a hadron collider.

This leads to an intriguing possibility. Colored technipions may be produced and observed at the LHC (or another high-energy hadron collider). Because they are produced strongly, there may be no way to infer that they are in fact technipions and are associated with electroweak symmetry breaking sector. However, the *combination* of their discovery with the observation of a large number of gauge-boson pairs may permit us to deduce that the colored scalars are PNGB's of the symmetry breaking sector [60].

The contribution of loops of colored technipions to the production of gauge-boson pairs through gluon fusion was calculated to leading order in chiral perturbation theory in ref. 59. Unfortunately, general considerations [61] show that in theories with many Goldstone bosons, chiral perturbation theory breaks down at very low energies. In the one-family model, for example, chiral perturbation theory breaks down at a scale of order 440 GeV! This precludes the possibility of making accurate predictions of the number of $ZZ$ and $WW$ events in such a theory and, for this reason, we refrain from reporting a specific number of events.

Nonetheless, the number of events expected is quite large. In Figure 4 we plot the $ZZ$ differential cross section as a function of $ZZ$ invariant mass at the LHC in a toy $O(N)$ scalar-model [60]. The parameters of the $O(N)$ model were chosen so that the size of signal is representative of what one might expect in a one-family technicolor model. Note that there are almost an order of magnitude more events due to gluon fusion than due to the continuum $q\bar{q}$ annihilation for $ZZ$ invariant masses between 300 GeV and 1 TeV. The observation of such a large two gauge-boson pair rate at a hadron collider would be compelling evidence that the EWSB sector couples to color.

## 4.5   Enhancement of $t\bar{t}$ production

The $\bar{t}t$ production rate and associated pair–mass and momentum distributions measured in Tevatron Collider experiments may probe flavor physics that lies beyond the standard model. Top–quark production can be significantly modified from QCD expectations by the resonant production of scalar or vector particles with masses of order $400 - 500$ GeV. Such particles naturally arise in many models of electroweak symmetry and flavor physics. The effects of both colored and colorless resonances have recently been studied in detail [62, 63].

The color–octet technipion, $\eta_T$, expected to occur in multiscale models [16] of walking technicolor [10] can easily double the $\bar{t}t$ rate. In general, an $\eta_T$ occurs in technicolor models which have color–triplet techniquarks [24, 42]. The production in hadron collisions via gluon fusion of a "standard" $\eta_T$—the one occurring in a one-family technicolor model and having decay constant $F = 123$ GeV and nominal couplings to quarks and gluons—has been shown [44, 62, 64] to increase the $\bar{t}t$ rate
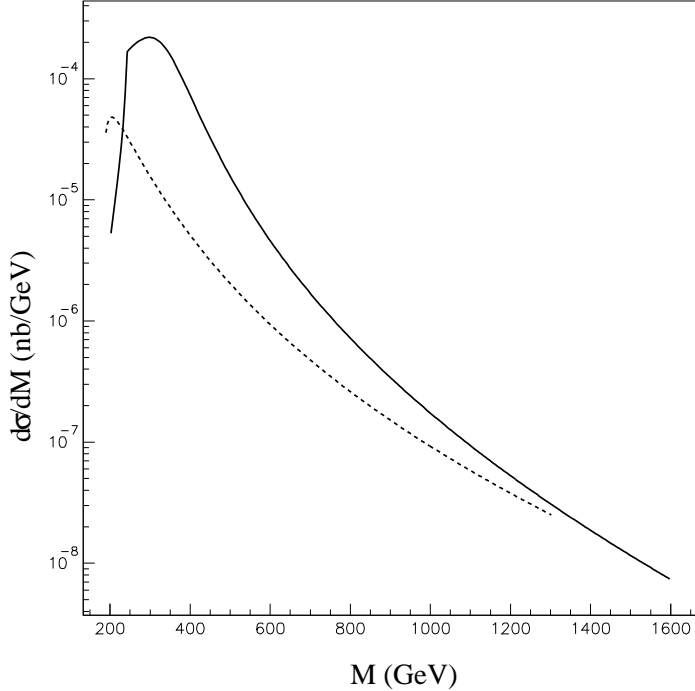
Figure 4:   The $ZZ$ differential cross section in nb/GeV vs. $M_{ZZ}$ in a toy $O(N)$ scalar-model with three color-octet PNGBs (solid curve), and the continuum $q\bar{q}$ annihilation background (dashed curve). A pseudo-rapidity cut $|\eta| < 2.5$ is imposed on the final state $Z$'s. From ref. 57.

by only 15% . Because of uncertainties in QCD corrections to the standard model $\bar{t}t$ rate, this is unlikely to be observable. In multiscale models, however, the $\eta_T$ decay constant is much smaller, $F \sim 20 - 40$ GeV. For $M_{\eta_T} = 400 - 500$ GeV, this small decay constant produces a measurably larger $\bar{t}t$ rate. We illustrate this effect in Figure 5.

To understand why multiscale technicolor implies a much larger $\eta_T \to \bar{t}t$ rate, consider $\sigma(p\bar{p} \to \eta_T \to \bar{t}t)$. For a relatively narrow $\eta_T$, it is given by

$$\sigma(p\bar{p} \to \eta_T \to \bar{t}t) \simeq \frac{\pi^2}{2s} \frac{\Gamma(\eta_T \to gg) \ \Gamma(\eta_T \to \bar{t}t)}{M_{\eta_T} \ \Gamma(\eta_T)} \int_{-Y_B}^{Y_B} dy_B \ z_0 \ f_g^{(p)}(\sqrt{\tau}e^{y_B}) \ f_g^{(p)}(\sqrt{\tau}e^{-y_B}) \ .$$

(32)

Here, $f_g^{(p)}$ is the gluon distribution function in the proton, $\tau = M_{\eta_T}^2/s$, $y_B$ is the boost rapidity of the subprocess frame, and $z_0$ is the maximum value of $z = \cos\theta$
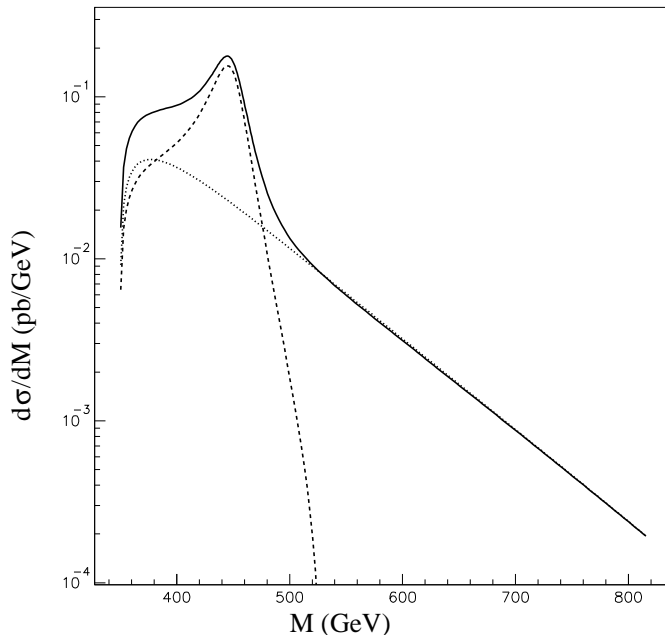
20

Figure 5: The $\bar{t}t$ invariant mass distribution in the presence of an $\eta_T$, in $\bar{p}p$ collisions at $E_{cm} = 1800$ GeV, for $m_t = 175$ GeV and $M_{\eta_T} = 450$ GeV, $F_Q = 30$ GeV and $C_t = -1/3$. The QCD (dotted curve), $\eta_T \to \bar{t}t$ and its interference with the QCD amplitude (dashed), and total (solid) rates have been multiplied by 1.62 to take higher order corrections into account. No rapidity cut is applied to the top quarks. From ref. 64.

allowed by kinematics and fiducial cuts [44]. The decay widths of the $\eta_T$ are essentially those given for $P_8^{0\prime}$ widths in section 4.1 – though the factor of $\frac{3}{16\pi}$ in equation (19) is more generally $\frac{C_q^2}{16\pi}$ where $C_q$ depends on the details of the ETC model. The key point here is that, unless $C_q$ is less than about 0.2 for the top quark, the cross section is simply proportional to $\Gamma(\eta_T \to gg)$ and the form of this decay rate is fairly model-independent: it depends only on the technicolor and color representations of the $\eta_T$ and on $F^{-2}$. Thus, the small decay constant of the $\eta_T$ in multiscale technicolor implies a large $\sigma(p\bar{p} \to \eta_T \to \bar{t}t)$ [62].

If an $\eta_T$ with multiscale dynamics produces an excess of $\bar{t}t$ events, then there also must be color–octet technirhos, $\rho_T$, which have flavor–blind couplings to quarks and gluons. The models discussed in [16, 37] indicate that they have mass in the

21

range $200 - 600$ GeV, making them potentially accessible to the Tevatron. If the technirhos decay primarily to pairs of technipions, the latter may be sought via their expected decays to heavy quarks and leptons. On the other hand, it is quite possible that at least one of these $\rho_T$ decays predominantly into $gg$ and $\bar{q}q$. If techni-isospin breaking is appreciable, the $\rho_T$ will be approximately ideally mixed states $\rho_{UU}$ and $\rho_{DD}$. In this case, a $\rho_{DD}$ decaying primarily to dijets can be seen either as a resonance in the dijet invariant mass distribution or (assuming good b-jet identification and reconstruction efficiency) a more prominent resonance in the $b\bar{b}$ distribution. If techni-isospin breaking is small, the $\rho_T$ will be more difficult to see [62].

More generally, many models of the relationship between the top quark and electroweak symmetry breaking (e.g. models with technicolor, top condensation [66], or extra gauge bosons) suggest the possibility of new color-singlet or color-octet vector resonances coupling strongly to the top quark. A recent study of the effects of such resonances on $\bar{t}t$ production is quite encouraging. Resonances as heavy as $700 - 800$ GeV can increase the total production cross-section, alter the $\bar{t}t$ invariant mass distribution (e.g. by the visible presence of a resonance) and noticeably distort the $p_T$ distributions for either the W or the top quark (typically by adding more events at higher $p_T$). It appears that a sample of as few as 100 top quarks could be very informative. These ideas are discussed in greater detail in ref. 67.

# 5   Production Rates and Signatures in $e^+e^-$ Machines

## 5.1   Neutral PNGBs

The lightest of the PNGBs will be neutral under both color and electromagnetism. If light enough, a neutral PNGB can be singly produced at LEP via an ABJ anomaly [68] coupling to pairs of electroweak gauge bosons. While early studies [69] underestimated the rate of PNGB production at the $Z$ resonance, later work [70] showed that the relevant $Z$ branching rates can be large enough to render these particles visible. Here, we summarize the possibilities at LEP, LEP II and hadron colliders for detecting neutral PNGBs. Since a given model may have several neutral PNGBs (e.g. the one-family technicolor model has both $P^0$ and $P^{0\prime}$), we denote these particles collectively as $\phi$ in this section.

The dominant decay mode of a PNGB in a given technicolor model depends both on the gauge couplings of the technifermions and on any interactions coupling technifermions to ordinary fermions. A neutral colorless PNGB produced by $Z$-decay can certainly decay to an off-shell $Z$ plus another electroweak gauge boson (photon or $Z$). It may also be able to decay to a pair of photons; if allowed, this

mode dominates over decays via off-shell $Z$'s. If some technifermions are colored, the PNGB may have an anomaly coupling allowing it to decay to gluons. If the PNGB gets its mass from effective four-fermion interactions (e.g. due to extended technicolor), then it will be able to decay to an $f\bar{f}$ pair. Finally, in some models, the PNGB may decay dominantly to particles in an invisible sector.

The dominant production mode for a PNGB at LEP is generally the $Z \to \gamma\phi$ process, for which the rate is:

$$\Gamma(Z \to \gamma\phi) = 5.7 \times 10^{-6} \text{GeV} \left(\frac{246\text{GeV}}{F}\right)^2 (N_{TC}A_{\phi Z\gamma})^2 \left(1 - \frac{M_\phi^2}{M_Z^2}\right)^3 \qquad (33)$$

where $F$ is the techni-pion decay constant, $N_{TC}$ is the number of technicolors, and $A_{\phi Z\gamma}$ is proportional to the anomaly factor $S_{PB_1B_2}$ discussed earlier

$$S_{\phi Z\gamma} = 2\sqrt{2}gg'N_{TC}A_{\phi Z\gamma} \quad . \qquad (34)$$

Clearly the rate depends heavily on the mass of the PNGB, the size of the technicolor gauge group and the strength of the anomaly coupling. It can easily vary from a value which is highly visible at LEP ($10^{-5}$ GeV) to one which is essentially invisible ($10^{-7}$ GeV or less).

LEP searches for neutral PNGBs ($\phi$) in the $Z \to \gamma\phi$ channel can exploit all the possible decay modes [70, 71]. The three photon final state would provide a dramatic signal of non-standard physics. If it occurred at a rate greater than $10^{-5}$, the sheer number of events would indicate the presence of non-standard physics. If it occurred at a lower rate, the distinctive kinematics of the signal could still distinguish it from background. The final states with missing energy plus photon(s) would be a definite indication of new physics because of the negligible standard model background. Finally, while the large background would probably make jets plus photon the hardest signal to extract, isolation and minimum energy cuts should make this feasible as well.

A $Z \to \gamma\phi$ decay rate of approximately $2 \times 10^{-6}$ GeV would be required to make the PNGB potentially visible in a sample of $10^7$ $Z$ bosons. For a model with given values of $F$, $N$ and $A_{\phi Z\gamma}$, the mass of the heaviest PNGB for which the decay rate achieves that size is

$$M_\phi < 91\text{GeV}\sqrt{1 - \left(\frac{(F/123\text{GeV})}{3.3N_{TC}A_{\phi Z\gamma}}\right)^{\frac{2}{3}}}. \qquad (35)$$

We can use the values of the anomaly factors for $P^0$ and $P^{0\prime}$ quoted earlier in Table 7 to evaluate this mass bound in the one-family technicolor model. For the isosinglet PNGB $P^{0\prime}$

$$M_{P^{0\prime}} < 91\text{GeV}\sqrt{1 - \left(\frac{6.9}{N_{TC}}\right)^{\frac{2}{3}}} \qquad (36)$$

so that for $N_{TC} = 7$ the $Z$ would radiatively decay to an 8 GeV $P^{0\prime}$ with a large enough rate, while for $N_{TC} = 8$ the $Z$ would decay with a sufficiently large rate to a $P^{0\prime}$ as heavy as 28 GeV. The $Z$ decay to the isotriplet $P^0$, on the other hand, would have a tiny rate for technicolor groups of this size, because the anomaly factor is proportional to $(1 - 4\sin^2\theta)$.

A large $Z \to \gamma\phi$ decay rate is necessary but not sufficient to ensure visibility: various cuts must also be employed to distinguish signal from background. A more detailed analysis [70, 71] demonstrates that LEP experiments can expect to detect PNGBs of masses up to about 65 GeV (e.g. in models with a larger $Z \to \gamma\phi$ decay rate than in one-family technicolor with small N). Note that this is substantially higher than the mass of the heaviest color-neutral electrically-charged PNGB accessible to LEP – the kinematic limit for charged particles is $M_Z/2$.

Two factors enhance the PNGB signal relative to the standard model background at LEP. The final state is two-body while the background generally requires the direct production of at least three final-state particles. And the signal is a (rare) decay of the $Z$ resonance while the dominant background is non-resonant. The second of these advantages will be missing at higher-energy electron-positron colliders, where the PNGB will instead be produced through off-shell $Z$'s or photons. This is sufficient to render the PNGB essentially invisible at LEP II or an NLC. Though the signal events would still be striking, there will be too few, both in absolute terms and relative to the backgrounds, to allow detection. The preceding remarks may be modified in multiscale models, where the anomalous coupling can be enhanced by the smaller value of $F$, increasing the number of events at higher-energy electron-positron colliders [75].

The possibility of detecting the PNGB in the $Z \to f\bar{f}\phi$ channel at LEP has also been considered, but this is far less promising. If the $f\bar{f}$ pair is produced through an intermediate photon or off-shell $Z$, the branching ratios are generally less than $10^{-7}$, rendering these modes invisible [71, 72]. If extended-technicolor-like four-fermion interactions allow the PNGB to couple directly to fermions, then $Z \to f\bar{f}\phi$ can proceed via a diagram with a propagating fermion $f$ (or $\bar{f}$). Assuming the PNGB coupling to fermions were proportional to the fermion mass, $Z \to b\bar{b}\phi$ could have a branching ratio as large as $10^{-6}$; however in this case, the PNGB would also decay mostly to jets, yielding a four-jet final state that could be difficult to disentangle from standard model background [71].

## 5.2   Other particles

Electrically charged PNGBs whether colored or color-neutral [$P^\pm$, $P_3^\pm$, $P_8^\pm$] may be pair-produced at electron-positron colliders so long as their mass does not exceed the kinematic limit of $\sqrt{s}/2$. Presumably these particles can also be detected essentially up to the kinematic limit. The current lower bound on the mass of colorless electrically charged PNGBs from OPAL data is 35 GeV [74].

Certain resonances can be detected through their effects on the process $e^+e^- \to W_L^+ W_L^-$ [77], as discussed in ref. 5. For models in which the longitudinal components of the $W$ and $Z$ are strongly self-interacting, one must include rescattering processes when computing electroweak gauge boson pair production [76]. The high energy behavior of the spin I and isospin J scattering amplitude $V_L V_L \to V_L V_L$ ($V = W, Z$) can be modeled by including resonances with the appropriate quantum numbers. For example, it is claimed [77] that vector resonances of masses up to 4 TeV in models with $F = 246$ GeV can be probed in this way at a $\sqrt{s} = 1.5$ TeV $e^+e^-$ collider. An $e^+e^-$ machine of similar or lower energy should be able to decisively test multiscale models since such models have smaller values of $F$ and predict lighter vector resonances.

Finally, additional studies are possible if one runs an $e^+e^-$ machine as a $\gamma\gamma$ collider by employing inverse Compton scattering of a high-powered laser beam off the fermion beams. In this case, one could study the reactions $\gamma\gamma \to (P^0, P^{0\prime}, P^+P^-, P_8^+ P_8^-)$ and $\gamma g \to (P_8^0, P_8^{0\prime})$, where the gluon in the second process comes from one of the photons. The single $P^0$ and $P^{0\prime}$ production is similar to standard model Higgs production, which has been studied in ref. 73. Unless $F$ is much smaller than $v = 246$ GeV, the partial widths for the $P^0$, $P^{0\prime}$ and Higgs to decay into $\gamma\gamma$ are of the same order of magnitude (for the same value of the scalar particle mass) and it will be difficult to distinguish among those scalars by a measurement of the partial width. This is in contrast with two Higgs doublets models or Minimal Supersymmetric Models, where the measurement of the $\gamma\gamma$ partial width of the scalar (or pseudoscalar) particle can put some constraints on the free parameters of the model. A detailed study of the processes mentioned above has not appeared in the literature.

# 6   Summary and Conclusion

In this report we have reviewed the characteristics of and constraints on realistic models of dynamical symmetry breaking. We have focused on properties of the extra colored pseudoscalars and vector particles generically predicted by such models. These are examples of particles associated with the electroweak symmetry breaking sector that can be *strongly produced* at hadron colliders. The phenomenology of strong scattering of longitudinally polarized electroweak gauge bosons and possible color singlet resonances (such as the techni-rho, techni-omega and techni-sigma) can be found in ref. 5. Similarly, the phenomenology of color-triplet scalar and vector particles that arise in these models is analogous to that of leptoquarks and is covered in ref. 46, at least in the case where those particles decay to first- or second-generation fermions. In Table 10 we summarize the discovery reach of different machines.

A number of issues deserve further study. For example, we have said very

little about phenomenology of color-octet vector resonances. The only study of these states was performed in ref. 37 in the context of multiscale models (for the SSC), where optimistic assumptions about jet resolution were used. More detailed analyses of the LHC discovery reach for such particles are clearly necessary. On the topic of colored scalars and vectors in general, it would be natural to assume that they decay predominantly to *third*-generation fermions. We expect that such particles could be detected up to the kinematic limit at an $e^+e^-$ collider of sufficient luminosity. Using events with one or more tagged $t$-quark(s) should allow for substantial discovery reach in hadron colliders as well, but detailed detector-dependent studies will be required to evaluate this reach.

Finally, we note that in models where the technifermions *do not* carry color the ETC gauge-boson responsible for generating the top-quark mass *must* be colored and may be light enough to be pair-produced at the LHC. While this process has been studied at the parton-level at the SSC [78], further work is needed to understand the potential at the LHC.

Table 10: Discovery reach of different accelerators for particles associated with realistic models of a strong EWSB sector.

| Particle | Tevatron | LHC | LEP I | LEP II | TLC |
|---|---|---|---|---|---|
| $P^{0\prime}$ | — | $110 - 150$ GeV[a] | 8 GeV[b] ; 28 GeV[b] | —[c] | —[c] |
| $P^0$ | — | — | — | — | — |
| $P^+P^-$ | — | 400 GeV[d] | 35 GeV[e] | 100 GeV[f] | 500 GeV[f] |
| $P_8^{0\prime}(\eta_T)$ | $400 - 500$ GeV[g] | 325 GeV[h] | — | — | — |
| $P_8^0$ | $10 - 20$ GeV[h] | 325 GeV[h,i] | — | — | — |
| $P_8^+P_8^-$ | $10 - 20$ GeV[h,i] | 325 GeV[h,i] | 45 GeV[e] | 100 GeV[f] | 500 GeV[f] |
| $P_3^+P_3^-$ | —[i] | —[i] | — | 100 GeV[f] | 500 GeV[f] |

[a] Decay mode $P^{0\prime} \to \gamma\gamma$ , similar to a light neutral Higgs [79].

[b] Decay mode $Z \to \gamma P^{0\prime}$, assuming a one-family model, with $N_{TC} = 7$ and $N_{TC} = 8$ respectively; no reach for $N_{TC} < 7$; for larger $Z\gamma P^{0\prime}$ couplings, the discovery reach extends to 65 GeV [70, 71, 72].

[c] No reach for one-family model; possibility of reach for the Lane-Ramana [37] multiscale model in the processes $e^+e^- \to P\gamma$ , $Pe^+e^-$ [75]. The discovery reach could be greatly improved if the TLC operates in a $\gamma\gamma$ mode.

[d] Estimated from work on charged Higgs detection (via $gb \to tH^- \to t\bar{t}b$) for $\tan\beta \simeq 1$, $m_t = 180$ GeV, 100 fb$^{-1}$ integrated luminosity and assuming a $b$-tagging efficiency $\epsilon_b = 0.3$ [80].

[e] Current OPAL limit [74]. The kinematic limit is $M_Z/2$.

[f] Kinematical limits for LEP200 and a 1 TeV $e^+e^-$ collider (TLC) [81].

[g] Contribution to the $\bar{t}t$ cross section in multiscale models [62].

[h] QCD pair production of colored PNGBs with decay into 4 jets [55].

[i] QCD pair production of colored PNGBs, each decaying to $t\bar{t}$, $t\bar{b}$, $t\tau$ or $t\nu_\tau$ should allow higher reach in mass. This has yet to be studied.

# Acknowledgements

# References

[1] G. 't Hooft, in *Recent Developments in Gauge Theories*, G. 't Hooft, *et al.*, eds., (Plenum Press, New York 1980).

[2] K. G. Wilson, *Phys Rev.* **B4** (1971) 3184; K. G. Wilson and J. Kogut, *Phys. Rep.* **12** (1974) 76.

[3] L. Susskind, *Phys. Rev.* **D20** (1979) 2619; S. Weinberg, *Phys. Rev.* **D13** (1976) 974, and *Phys. Rev.* **D19** (1979) 1277.

[4] K. Lane, Boson U. preprint BUHEP-94-2, to appear in *1993 TASI Lectures* (World Scientific, Singapore); S. King, Southampton preprint SHEP 93/94-2, hep-ph/9406401; M. Einhorn *Perspectives on Higgs Physics*, G. Kane ed. (World Scientific, Singapore 1993) 429.

[5] Report of the "Strongly Coupled Electroweak Symmetry Breaking: Model Independent Results" subgroup of the "Electroweak Symmetry Breaking and Beyond the Standard Model" working group of the DPF Long Range Planning Study. T. Han, M. Golden and G. Valencia, convenors.

[6] S. Dimopoulos and L. Susskind, *Nucl. Phys.* **B155** (1979) 237.

[7] E. Eichten and K. Lane, *Phys. Lett.* **B90** (1980) 125.

[8] J. Ellis, M. K. Gaillard, D. V. Nanopoulos and P. Sikivie, *Nucl. Phys.* **B182** (1981) 529; S. Dimopoulos and J. Ellis, *Nucl. Phys.* **B182** (1981) 505.

[9] S. Weinberg, *Physica* **96 A** (1979) 327; H. Georgi and A. Manohar, *Nucl. Phys.* **B234** (1984) 189.

[10] B. Holdom, *Phys. Rev* **D24** (1981) 1441; B. Holdom, *Phys. Lett.* **B150** (1985) 301; K. Yamawaki, M. Bando, and K. Matumoto, *Phys. Rev. Lett.* **56** (1986) 1335; T. Appelquist, D. Karabali, and L.C.R. Wijewardhana, *Phys. Rev. Lett. 57* (1986) 957; T. Appelquist and L.C.R. Wijewardhana, *Phys. Rev*

**D35** (1987) 774; T. Appelquist and L.C.R. Wijewardhana, *Phys. Rev* **D36** (1987) 568.

[11] S. Glashow, J. Illiopoulos, and L. Maiani, *Phys. Rev* **D2** (1970) 1285.

[12] S. Dimopoulos, H. Georgi, and S. Raby, *Phys. Lett.* **B127** (1983) 101; S.-C. Chao and K. Lane, *Phys. Lett.* **B159** (1985) 135; R.S. Chivukula and H. Georgi, *Phys. Lett.* **B188** (1987) 99.

[13] P. Sikivie *et al.*, *Nucl. Phys.* **B173** (1980) 189; R. Renkin and M. Peskin *Nucl. Phys.* **B211** (1983) 93; T. Appelquist *et al.*, *Phys. Rev.* **D31** (1985) 1676; R. S. Chivukula, *Phys Rev. Lett.* **61** (1988) 2657; B. Holdom *Phys. Lett.* **B226** (1989) 137; T. Appelquist *et al.*, *Phys. Lett.* **B232** (1989) 211; H. Goldberg *Phys. Rev. Lett.* **58** (1987) 633.

[14] R. S. Chivukula, K. Lane, and A. G. Cohen, *Nucl. Phys.* **B 343** (1990) 554; T. Appelquist, J. Terning, and L. Wijewardhana, *Phys. Rev* **44** (1991) 871.

[15] T. Appelquist, M. Einhorn, T. Takeuchi, and L.C.R. Wijewardhana, *Phys. Lett.* **220B**, 223 (1989); V.A. Miransky and K. Yamawaki, *Mod. Phys. Lett.* **A4** (1989) 129; K. Matumoto *Prog. Theor. Phys. Lett.* **81** (1989) 277.

[16] K. Lane and E. Eichten, *Phys. Lett.* **B222** (1989) 274.

[17] B. Holdom, *Phys. Rev. Lett.* **60** (1988) 1233; T. Appelquist and O. Shapira, *Phys. Lett.* **B249** (1990) 327.

[18] B. Lynn, M. Peskin, and R. Stuart, in *Physics at LEP*, J. Ellis and R. Peccei eds. CERN preprint **86-02** (1986). M. Golden and L. Randall, *Nucl. Phys.* **B361**, 3 (1991); B. Holdom and J. Terning, *Phys. Lett* **B247**, 88 (1990); M. Peskin and T. Takeuchi, *Phys. Rev. Lett.* **65**, 964 (1990); A. Dobado, D. Espriu, and M. Herrero, *Phys. Lett.* **B253**, 161 (1991); M. Peskin and T. Takeuchi *Phys. Rev.* **D46** 381 (1992).

[19] M. Dugan and L. Randall, *Phys. Lett.* **B264** (1991) 154; M. Luty and R. Sundrum, *Phys. Rev. Lett.* **70** (1993) 529.

[20] B. Holdom *Phys. Lett.* **B259** (1991) 329; E. Gates and J. Terning *Phys. Rev. Lett.* **67** (1991) 1840; T. Appelquist and G. Triantaphyllou, *Phys. Lett.* **B278** (1992) 345; R. Sundrum and S. Hsu, *Nucl. Phys.* **B391** (1993) 127; N. Evans and D. Ross, *Nucl. Phys.* **B417** (1994) 151.

[21] T. Appelquist and J. Terning, *Phys. Lett.* **B315** (1993) 139.

[22] R. S. Chivukula, S. B. Selipsky, and E. H. Simmons, *Phys. Rev. Lett.* **69** (1992) 575; E H. Simmons, R S. Chivukula and S B. Selipsky, in proceedings of *Beyond the Standard Model III*, S. Godfrey and P. Kalyniak, eds., (World Scientific, Singapore, 1993); N. Kitazawa *Phys. Lett.* **B313** (1993) 395 ; R. S. Chivukula, E. Gates, E. H. Simmons, and J. Terning, *Phys. Lett.* **B311** (1993) 157.

[23] N. Evans, U. of Wales, *Phys. Lett.* **B331** (1994) 378, hep-ph/9403318.

[24] E. Farhi and L. Susskind, *Phys. Rev.* **D20** (1979) 3404.

[25] B. Holdom, *Phys. Rev.* **D23** (1981) 1637.

[26] H. Georgi and S. Glashow, *Phys. Rev. Lett.* **47** (1981) 1511.

[27] J. Ellis and P. Sikivie, *Phys. Lett.* **B104** (1981) 141.

[28] S. King, *Phys. Lett.* **B105** (1981) 182.

[29] A. Buras, S. Dawson, and A. Schellekens, *Phys. Rev.* **D27** (1983) 1171.

[30] R. S. Chivukula, H. Georgi, and L. Randall, *Nucl. Phys.* **B292** (1987) 93; R. S. Chivukula and H. Georgi, *Phys. Rev.* **D36** (1987) 2102; V. Bhansali and H. Georgi, *Phys. Lett.* **B197** (1987) 553; A. Nelson *Phys. Rev.* **D38** (1988) 2875.

[31] D.-X. Li, *Phys. Lett.* **B191** (1987) 369.

[32] E. Simmons, *Nucl. Phys.* **B312** (1989) 252; C. Carone and E. Simmons, *Nucl. Phys.* **B397** (1992) 591; C. Carone and H. Georgi, *Phys. Rev.* **D49** (1994) 1427, hep-ph/9308205.

[33] H. Georgi, *Nucl. Phys.* **B307** (1988) 365; *Phys. Lett.* **B216** (1989) 155; J. Chay and E. Simmons, *Nucl. Phys.* **B315** (1989) 541.

[34] S. King, *Phys. Lett.* **B229** (1989) 253. S. King and S. Mannan, *Nucl. Phys.* **B369** (1992) 119.

[35] B. Holdom, *Phys. Lett.* **B143** (1984) 227; *Phys. Rev. Lett.* **57** (1986) 2496; *Phys. Rev. Lett.* **58** (1987) 177(E); *Phys. Lett.* **B246** (1990) 169; *Proc. Conf. Dynamical Symmetry Breaking, Nagoya 1991* (World Scientific, Singapore, 1991) 275.

[36] S. Dimopoulos and S. Raby, *Nucl. Phys.* **B192** (1981) 353; S. Samuel, *Nucl. Phys.* **B347** (1990) 625; A. Kagan and S. Samuel, *Phys. Lett.* **B252** (1990) 605.

[37] K. Lane and M.V. Ramana, *Phys. Rev.* **D44** (1991) 2678.

[38] G. Giudice and S. Raby,*Nucl. Phys.* **B368** (1992) 221.

[39] R. Sundrum, *Nucl. Phys.* **B395** (1993) 60.

[40] L. Randall, *Nucl. Phys.* **B403** (1993) 122.

[41] B. Holdom *Phys. Lett.* **B314** (1993)89.

[42] T. Appelquist and J. Terning, *Phys. Rev.* **D50** (1994) 2116.

[43] R. S. Chivukula, E. Simmons, and J. Terning, *Phys. Lett.* **B331** (1994) 383.

[44] E. Eichten, I. Hinchliffe, K. Lane and C. Quigg, *Rev. Mod. Phys.* **56** (1984) 579; E. Eichten, I. Hinchliffe, K. Lane and C. Quigg, *Phys. Rev.* **D34** (1986) 1547.

[45] For an alternative formulation, see R. Casalbuoni, S. de Curtis, D. Dominici and R. Gatto, *Phys. Lett.* **B155** (1985) 95; *Nucl. Phys.* **B282** (1987) 235.

[46] Report of the "Exotica" subgroup of the "Electroweak Symmetry Breaking and Beyond the Standard Model" working group of the DPF Long Range Planning Study. A. Djouadi, J. Ng and T. Rizzo, convenors.

[47] T. Das, *et al.*, *Phys Rev. Lett.* **18** (1967) 759.

[48] M. Peskin, *Nucl. Phys.* **B175** (1980) 197; J. Preskill, *Nucl. Phys.* **B177** (1981) 21.

[49] R. Dashen, *Phys. Rev.* **183** (1969) 1245.

[50] S. Dimopoulos, *Nucl. Phys.* **B168** (1980) 69; J. Ellis *et al.* in ref. 8; S. Dimopoulos, S. Raby and G. L. Kane, *Nucl. Phys.* **B182** (1981) 77 ; F. Hayot and O. Napoli, *Zeit. für Physik* **C7** (1981) 229.

[51] See, e.g., R. S. Chivukula and M. Golden, *Phys. Rev.* **D41** (1990) 2795.

[52] See, e.g., J. Ellis *et al.* in ref. 8.

[53] R. Rosenfeld and E.H. Simmons, work in progress.

[54] Z. Kunszt and W.J. Stirling, *Phys. Rev.* **D37** (1988) 2439.

[55] R.S. Chivukula, M. Golden and E.H. Simmons, *Nucl. Phys.* **B363** (1991) 83.

[56] S. Parke and T. Taylor, *Phys. Rev. Lett.* **56** (1986) 2459.

[57] M. Mangano and S. Parke, *Phys. Rev.* **D39** (1989) 758; M. Mangano and S. Parke, *Phys. Rep.* **200** (1991) 301; F.A. Berends, W.T. Giele and H. Kuijf, *Phys. Lett.* **B232** (1989) 266 and *Nucl. Phys.* **B333** (1990) 120.

[58] R. M. Harris, talk given at DPF-94, Albuquerque, August 2-6, 1994.

[59] J. Bagger, S. Dawson, and G. Valencia, *Phys. Rev. Lett.* **67**(1991), 2256 .

[60] R. S. Chivukula, M. Golden, and M. V. Ramana, *Phys. Rev. Lett.* **68** (1992), 2883.

[61] M. Soldate and R. Sundrum, *Nucl. Phys.* **B340** 1 (1990); R. S. Chivukula, M. Dugan, and M. Golden, *Phys. Rev.* **D47** (1993), 2930.

[62] E. Eichten and K. Lane, *Phys. Lett.* **B327** (1994) 129, hep-ph/9401236.

[63] C. T. Hill and S. J. Parke, *Phys. Rev.* **D49** (1994) 4454, hep-ph/9312324.

[64] T. Appelquist and G. Triantaphyllou, *Phys. Rev. Lett.* **69** (1992) 2750.

[65] K. Lane, Boston University preprint BUHEP-94-12, hep-ph/9406344.

[66] V.A. Miransky, M. Tanabashi, and K. Yamawaki, *Phys. Lett.* **B221** (1989) 177; V.A. Miransky, M. Tanabashi, and K. Yamawaki, *Mod. Phys. Lett.* **A4** (1989) 1043; Y. Nambu, EFI-89-08 (1989) unpublished; W.J. Marciano *Phys. Rev. Lett.* **62** (1989) 2793; W.A. Bardeen, C.T. Hill and M. Lindner, *Phys. Rev.* **D41** (1990) 1647; C.T. Hill, *Phys. Lett.* **B266** (1991) 419.

[67] Report of the "Top Quark as a Window on Electroweak Symmetry Breaking" subgroup of the "Electroweak Symmetry Breaking and Beyond the Standard Model" working group of the DPF Long Range Planning Study. M. Peskin and S. Parke, convenors.

[68] J.S. Bell and R. Jackiw, *Nuovo Cim.* **A60** (1969) 47; S.L. Adler, *Phys. Rev.* **117** (1969) 2526.

[69] J. Ellis. *et al.* in ref. 8; Z. Jian-zu, *Phys. Rev.* **D39** (1989) 354.

[70] A. Manohar and L. Randall, *Phys. Lett.* **B65** (1990) 537.

[71] L. Randall and E.H. Simmons, *Nucl. Phys.* **B380** (1992) 3.

[72] V. Lubicz, *Nucl. Phys.* **B404** (1993) 559

[73] D.L. Borden, D.A. Bauer and D.O. Caldwell, *Phys. Rev.* **D48** (1993) 4018.

[74] OPAL Collaboration, *Phys. Lett.* **B242** (1990) 299.

[75] V. Lubicz, private communication.

[76] F. Iddir, A. Le Yaouanc, L. Olivier, O. Pene and J. C. Raynal, *Phys. Rev.* **D41** (1990) 22; contributions by M. E. Peskin, T. Barklow and K. Hikasa in *Physics and Experiments with $e^+e^-$ Linear Colliders*, Saariselka, Finland, 1991; R. Orava, P. Eerola and M. Nordberg eds., World Scientific, Singapore 1992.

[77] T. Barklow, talk given at DPF-94, Albuquerque, August 2-6, 1994.

[78] P. Arnold and C. Wendt, *Phys. Rev.* **D33**, (1986) 1873.

[79] GEM Technical Design Report, **SSCL-SR-1219**, 1993.

[80] V. Barger, R. J. N. Phillips and D. P. Roy, *Phys. Lett.* **B324** (1994) 236, hep-ph/9311372; J. F. Gunion,*Phys. Lett.* **B322** (1994) 125, hep-ph/9312201.

[81] This is only an estimate, since the cross section falls as $\beta^3$ near the threshold. See, e.g., P. M. Zerwas, talk at LC92, *Workshop on $e^+e^-$ Linear Colliders*, Garmisch-Partenkirchen (FRG), 1992.